INVESTIGATION OF STRUCTURE AND PHASE COMPOSITION OF ALLOYS BASED ON THE Ti–Zr–Fe SYSTEM

V.F. KHORUNOV[1], **S.V. MAKSYMOVA**[1] and **G.M. ZELINSKAYA**[2]
[1]E.O. Paton Electric Welding Institute, NASU, Kiev, Ukraine
[2]G.V. Kurdyumov Institute for Metal Physics, NASU, Kiev, Ukraine

Melting temperature ranges for alloys of the Ti–Zr–Fe system were investigated, and liquidus surface of the ternary system in 2D and 3D graphic presentations was plotted. The eutectic pit comprising alloys that show promise for development of brazing filler metals was determined. Microstructure and morphological peculiarities of the alloys at different cooling rates were investigated. Filler metals for brazing titanium aluminides were developed on the basis of the investigation results.

Keywords: *brazing, filler metal, eutectic, structure, liquidus temperature, adhesion-active alloys, cooling rate, phase composition*

The basic system that shows promise for development of adhesion-active filler metals for brazing titanium alloys, including titanium aluminides, is the Ti–Zr system, which features formation of a continuous series of solid solutions. Alloying this system with other elements, such as manganese, iron and chromium, allows the melting temperature to be decreased to some extent owing to formation of low-temperature eutectics.

Alloying titanium with iron leads to formation of eutectic on the titanium side at a temperature of 1085 °C [1], while according to other references the temperature of the eutectic is 1100 °C. Solubility of iron in β-titanium is 22 at.%. The Zr–Fe system containing approximately 23 at.% Fe also has the low-temperature eutectic at a temperature of 928 °C between β-Zr and Zr_2Fe. Owing to their acceptable melting temperature range and good wettability, alloys of the Ti–Zr–Fe system are of interest for use as a base to develop filler metals for brazing titanium alloys, including intermetallic alloys. Unfortunately, the states of phase equilibrium in the Ti–Zr–Me ternary systems, which are good candidates for use as a base to develop filler metals, are little investigated so far.

The purpose of this study is to investigate adhesion-active alloys based on the Ti–Zr–Fe system, their melting temperature ranges and peculiarities of their structure formation at different cooling rates.

An experiment was designed to plot the liquidus surface of alloys of the Ti–Zr–Fe system. 36 experimental alloys of the Ti–Zr–Fe system marked by points in the diagram (Figure 1) were melted according to the experimental design. The contents of elements in the alloys were varied within the following ranges, at.%: 8.25–71.75 Zr, 6.0–79.75 Fe, and 4.0–76.75 Ti. Figure 1 also shows the binary diagrams according to [2].

Melting temperatures were determined by using differential thermal analyser VDTA-8M3 in BeO crucibles at a heating rate equal to 40 °C/min. The liquidus surface of the Ti–Zr–Fe ternary system* (Figure 2) was plotted by the experimental design simplex-lattice method [3–5], which is used to plot the liquidus surfaces of ternary systems bounded by two binary systems of the eutectic type and one system with a continuous series of solid solutions, as well as by using literature and experimental data (melting temperature range).

The eutectic pit can be seen on the 3D liquidus surface. The pit comprises eutectics with a minimal melting temperature, which is acceptable for their use as filler metals. A typical representative of such eutectic alloys is Ti–19Zr–20Fe with a melting temperature range of 940–960 °C, whose structure consists of solid-solution primary dendrites and eutectic (Figure 3, *a*).

Alloying the Ti–19Zr–20Fe alloy with aluminium (up to 11 %) and increasing the amount of zirconium by 8.5 % affect morphological peculiarities of the structure (Figures 3, *b* and 4). The primary phase enriched with zirconium and containing 21.5 % Fe and 15.26 % Al (Figure 4, Table 1, spectrum 1) was found to solidify in the form of dendrites. It is the main phase having a small amount of the Ti–22.5Zr–7.65Al–5.1Fe phase between the dendrites. The finely dispersed phase (Figure 4, Table 1, spectrum 3) with an increased content of zirconium (35.32 %) precipitates in the form of isolated white spot-like inclusions. This alloy differs from the previous compositions in brittleness.

It is a known fact that cooling rate has a high effect on structure formation of alloys, including the eutectic ones [6].

*The calculation procedure was developed by M.O. Karateev and V.V. Voronov.

© V.F. KHORUNOV, S.V. MAKSYMOVA and G.M. ZELINSKAYA, 2010

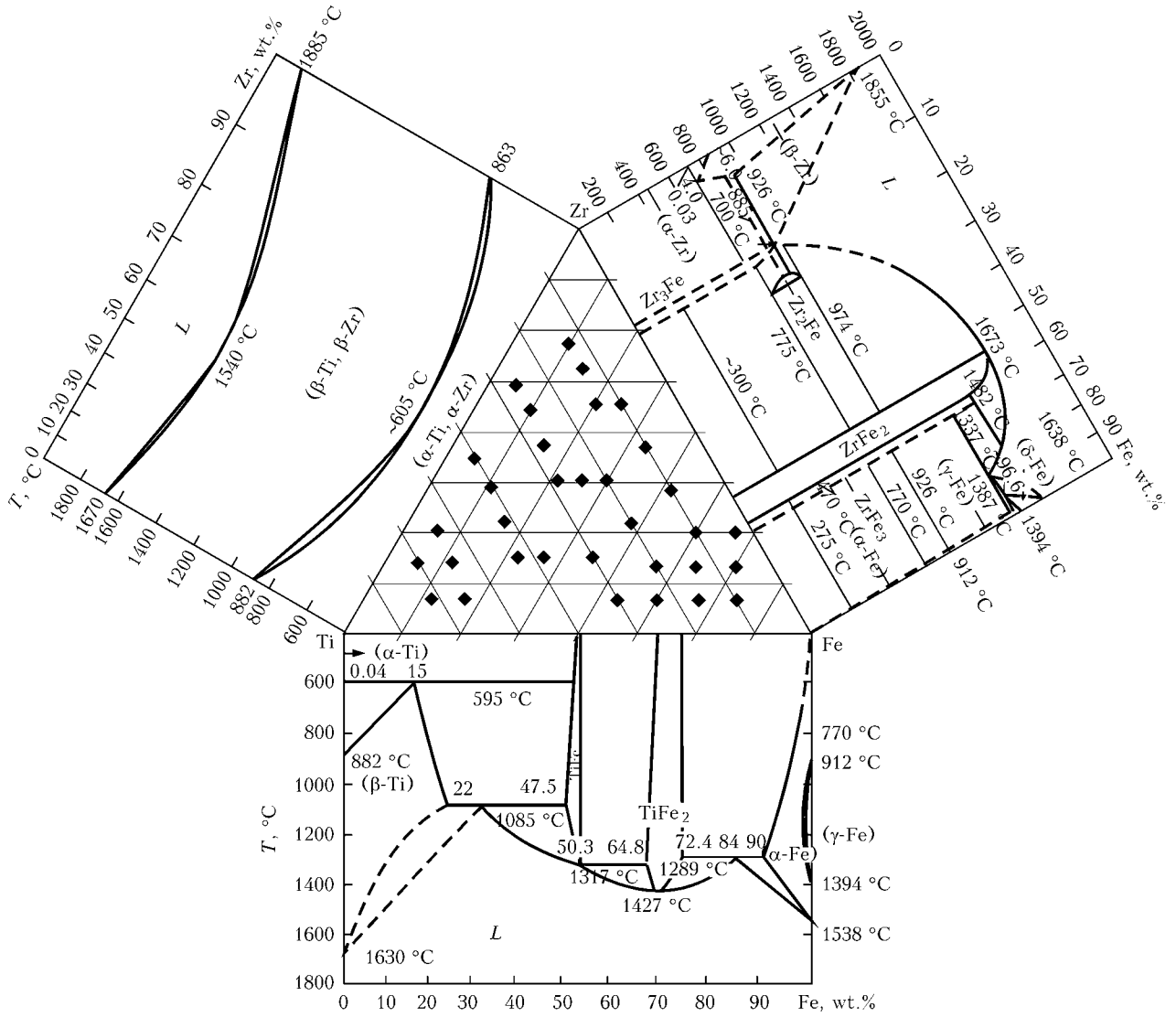

Figure 1. Positions of experimental alloys of the Ti–Zr–Fe system with adjoining binary diagrams

The said alloys were melted in a laboratory electric arc furnace on a copper water-cooled bottom plate.

The method of dispersion from liquid state (using electron beam heating) was used to provide a more homogeneous and finer structure of the alloys under investigation. The main point of the method is as follows. The metal melt is poured from the cold hearth onto a rotating drum mould, where it is built on to provide the required thickness of the skull [7, 8]. Then the drum mould with the skull is imparted a high rotation speed (about 2000 rpm), and the skull surface is melted with a concentrated electron beam. Under the effect of centrifugal forces, the molten metal is torn away in the form of a flow of liquid fine drops from the skull surface at a tangent to the focal spot of the concentrated electron beam. The flow of liquid drops of the melt, having a small diameter (about 1 mm) and high velocity (about 10 m/s), is directed to the shape-forming surface (mould). There the drops spread into a thin (about 0.1 mm) layer under the effect of the forward pressure and solidify with no formation of the molten pool. Some of them solidify in the form of spherical particles with a diameter of 1–3 mm, and others — in the form of particles of irregular shape.

Table 1. Chemical composition of calculated alloy Ti–27.5Zr–17.7Fe–11.4Al, at.%

Spectrum number	Al	Ti	Fe	Zr
1	15.26	33.51	21.50	29.73
2	7.65	64.76	5.10	22.50
3	9.39	43.57	11.72	35.32

The structure of the Ti–19Zr–20Fe alloy produced by electron beam remelting consists of rounded, coarse primary crystals of 73.8Ti–15.3Zr–10.9Fe (Figure 5, *a*) and eutectic, the main phase of which is the $(TiZr)_2Fe$ compound with a high atomic content of iron (31.23 %) (Figure 6, Table 2, spectrum 1). The second component of the eutectic is a phase with a chemical composition that is close to composition of the primary crystals (Figure 6, Table 2, spectrum 2). The degree of dispersion of structural components

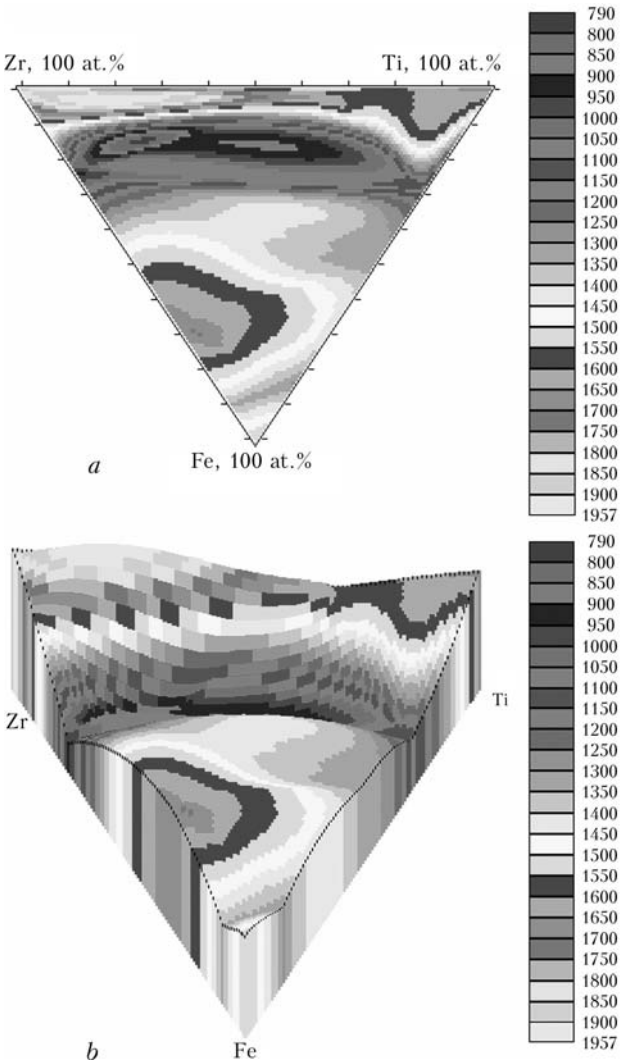

Figure 2. 2D (*a*) and 3D (*b*) picture of liquidus surface of alloys of the Ti–Zr–Fe system

grows with increase of the cooling rate (Figure 5, *b–f*). The cooling rate was determined by calculations in modelling of thermal processes occurring in rapid solidification of the dispersed melts [8, 9].

The structure of the alloy at a cooling rate of 10^2 °C/s differs from the previous one not only in size of the primary dendrites, but also in morphological peculiarities of the eutectic caused by a temperature gradient [6]. The smaller the diameter of spherical particles, the higher is the cooling rate, the smaller

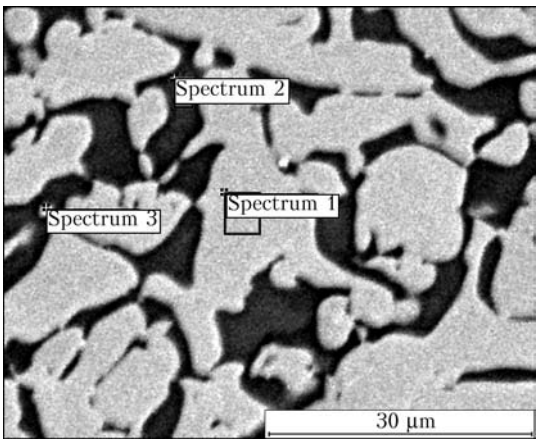

Figure 4. Microstructure and regions of chemical analysis of structural components of calculated alloy Ti–27.5Zr–17.7Fe–11.4Al

is the size of structural components of the eutectic, and the higher is the degree of its dispersion (Figure 5, *d*, *e*).

With further increase of the cooling rate to $6 \cdot 10^4$ °C/s, even in solidification of drops in the form of a thin strip, structural components of the alloy continue decreasing in size (Figure 5, *f*).

The use of super rapid quenching in the high-purity helium atmosphere allowed producing a homogeneous structure and uniform distribution of chemical components of the Ti–19Zr–20Fe filler metal in width of the strip (Figure 7, *a–d*). The cooling rate of the melt (i.e. the rate at the time point of solidification — formation of the strip) was estimated at $(2–5) \cdot 10^5$ °C/s. The strip can be used as an embedded element for brazing, which is very important, but it has an insufficient ductility. Even if it is in the amorphous state at the time point of solidification, a dramatic decrease of the cooling rate to $(2–5) \cdot 10^3$ °C/s after removing it from the disk may lead to partial crystallisation, and at the outlet it will be in the amorphous-crystalline state.

Results of X-ray diffraction analysis are in good agreement with metallographic examinations (Figures 8 and 9, *a*). The phases in solutions β-TiZr and $Fe(TiZr)_3$ were detected in X-ray pattern of the rapidly quenched Ti–19Zr–20Fe strip (diffractometer DRON-3, K_α radiation) against a background of the diffuse halo (Figure 8). It is a known fact that the

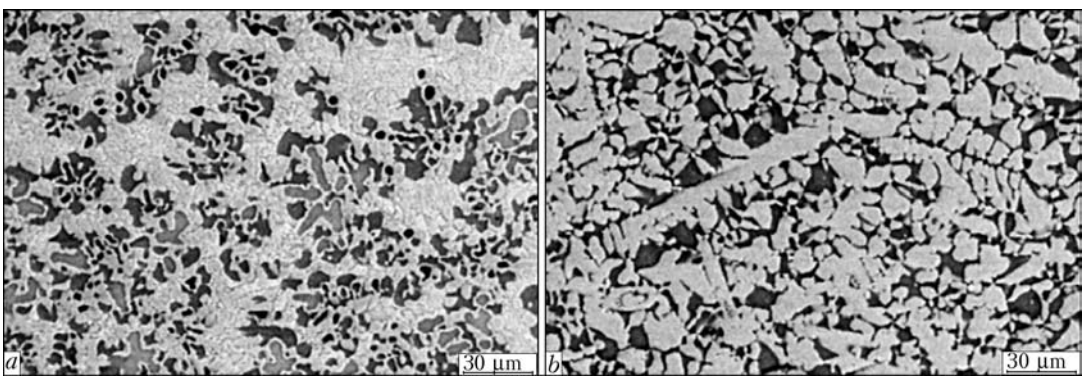

Figure 3. Microstructures of alloys Ti–19Zr–20Fe (*a*) and Ti–27.5Zr–17.7Fe–11.4Al (*b*) in as-cast condition

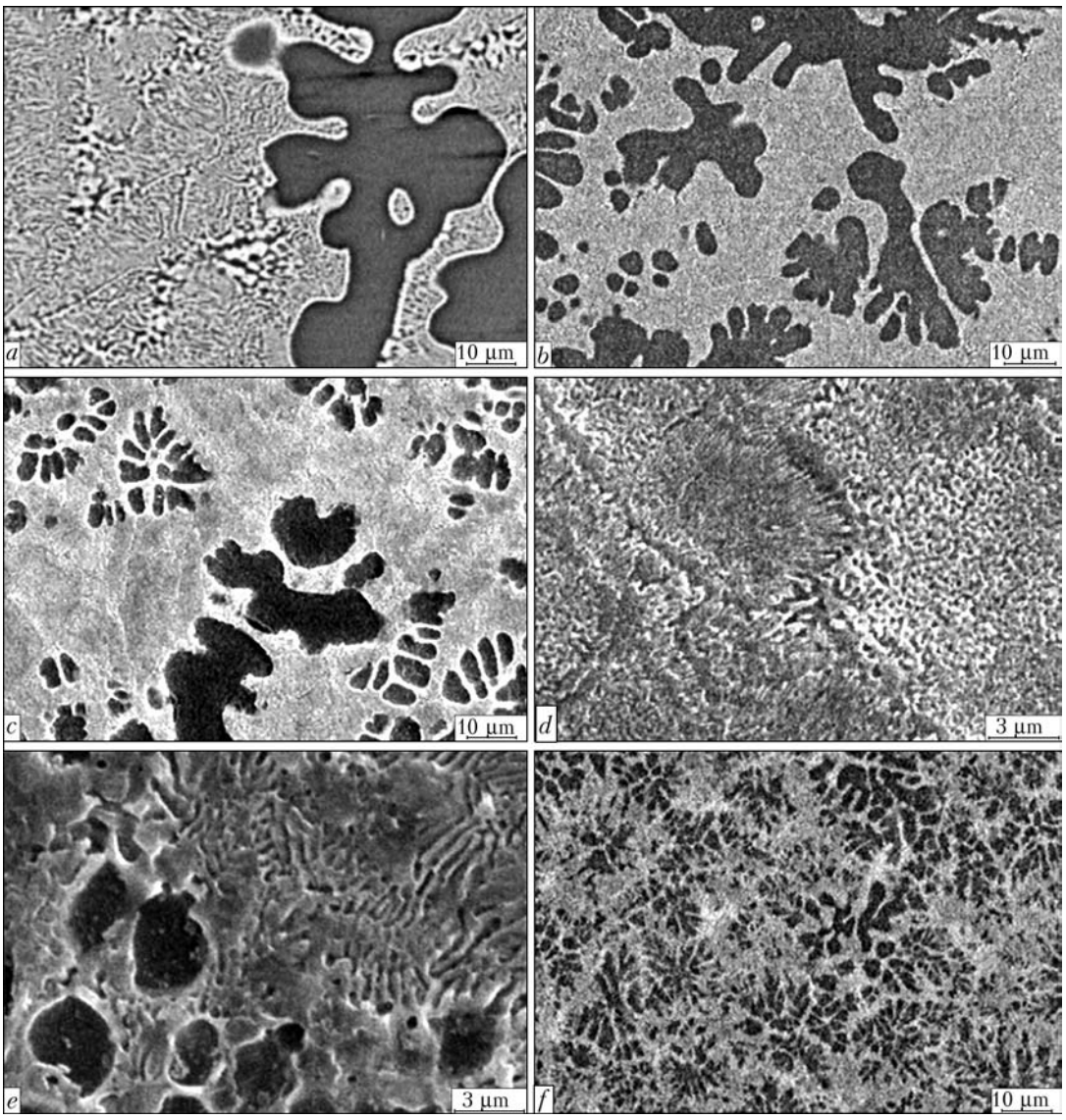

Figure 5. Microstructures of the Ti–19Zr–20Fe alloy produced at different cooling rates: *a* — v_{cool} = 2–5; *b–e* — $2 \cdot 10^2$; *f* — $6 \cdot 10^4$ °C/s

structure of the alloys is affected, in addition to the cooling rate, also by the melting parameters, such as time of holding of the molten pool, and its temperature at the time point of solidification (formation of strip). Other structural components may form in production of rapidly quenched strips under other conditions.

It should be noted that the parameter of height of structural factor $i(s)$ related to packing density of atoms is a very sensitive characteristic, which makes it possible to estimate the presence and content of the crystalline phase in the amorphous strip, this being associated with a number of technological factors taking place in production of amorphous strips from the melt [10]. Height of the structural factor (Figure 10) is a confirmation of the amorphous-crystalline state of the Ti–19Zr–20Fe alloy.

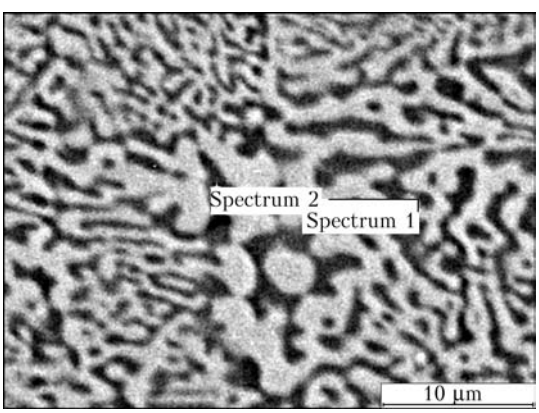

Figure 6. Microstructure and investigated regions of eutectic

As seen, a typical diffraction pattern in the form of diffuse maxima and a clearly defined effect with a split second maximum, which is always characteristic of amorphous materials [11], is observed for the Ti–27.5Zr–17.7Fe–11.4Al alloy strip (Figure 11). The

Table 2. Chemical composition of eutectic, at.%

Spectrum number	Ti	Fe	Zr
1	43.97	31.23	24.81
2	67.93	15.62	16.45

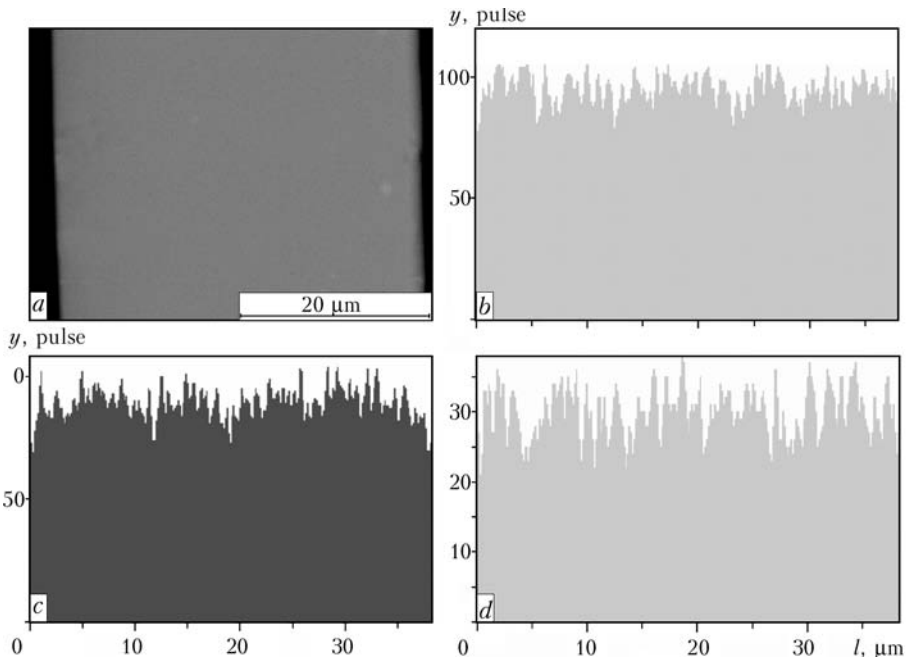

Figure 7. Microstructure of the Ti–19Zr–20Fe rapidly quenched strip (in reflected electrons) (*a*) and qualitative distribution of titanium (*b*), zirconium (*c*) and iron (*d*) in width of the strip along the scanning line

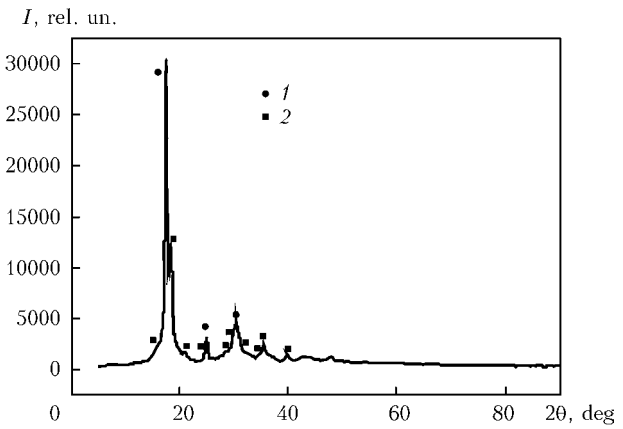

Figure 8. X-ray pattern of the Ti–19Zr–20Fe amorphous-crystalline strip: *1* — solution β-TiZr; *2* — solution $Fe(TiZr)_3$

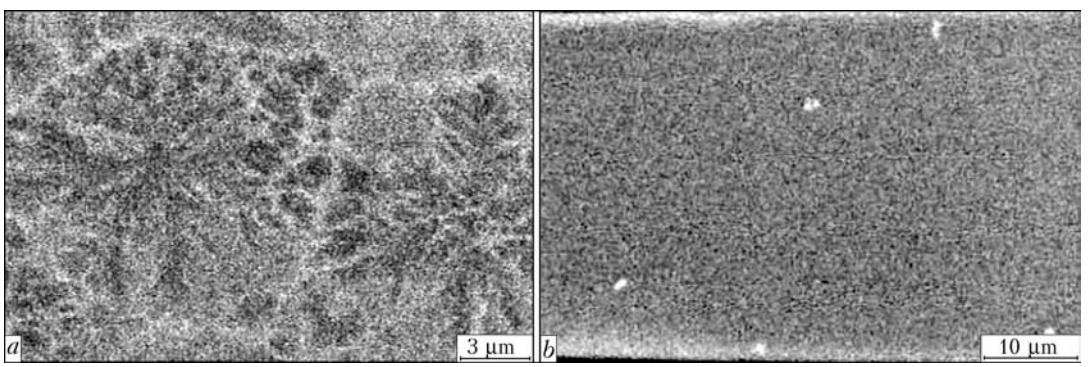

Figure 9. Microstructures of the Ti–19Zr–20Fe (*a*) and Ti–27.5Zr–17.7Fe–11.4Al (*b*) rapidly quenched strips

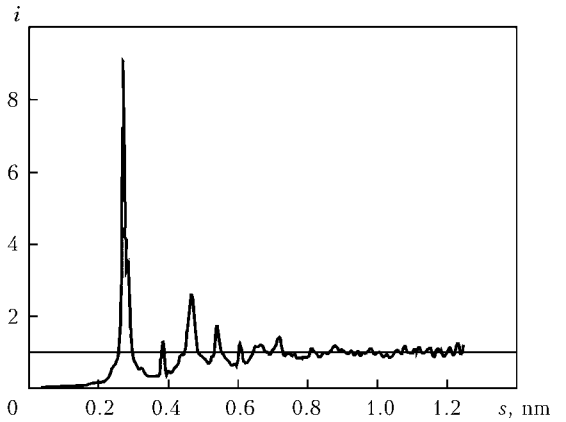

Figure 10. Structural factor of the Ti–19Zr–20Fe amorphous-crystalline strip

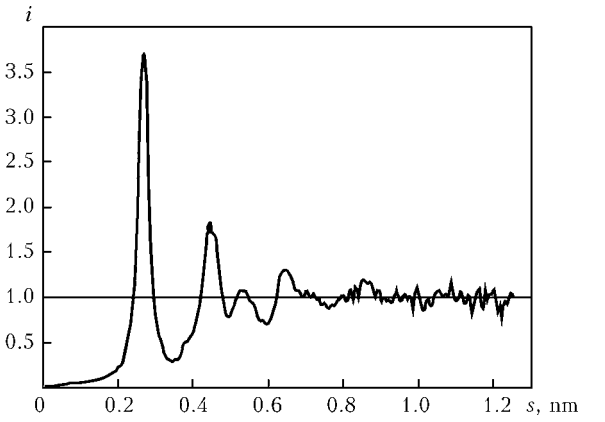

Figure 11. Structural factor of the Ti–27.5Zr–17.7Fe–11.4Al amorphous strip

rapidly quenched Ti–27.5Zr–17.7Fe–11.4Al alloy strip turned out to be amorphous (Figures 9, *b* and 11).

CONCLUSIONS

1. Alloys based on the Ti–Zr–Fe system were investigated within a wide concentration range. The plotted liquidus surface made it possible to find position of the eutectic pit, on which the alloys with a low melting temperature are located.

2. The Ti–19Zr–20Fe filler metal with a minimal solidus temperature was developed on the basis of the results obtained. It was determined that at a cooling rate increased to 10^2 °C/s the alloy structure consists of primary crystals of the 73.8Ti–15.3Zr–10.9Fe solid solution and eutectic.

3. Increasing the cooling rate (to 10^2 °C/s) of the Ti–19Zr–20Fe alloy in dispersion by electron beam melting leads to approximately 3–4 times decrease in size of its structural components.

4. The use of the super rapid quenching method ($v_{cool} = (2–5)\cdot10^5$ °C/s) provided a homogeneous strip of the Ti–19Zr–20Fe alloy in the amorphous-crystalline state. X-ray phase analysis showed the presence of the β-TiZr solid solution and $Fe(TiZr)_3$ phase.

1. (1997) *Constitutional diagrams of binary metallic systems*: Refer. Book. Vol. 2. Ed. by N.P. Lyakishev. Moscow: Mashinostroenie.
2. Massalski, T.B. (1990) *Binary alloy phase diagrams*. 2nd ed. Ohio: ASM Int., Materials Park.
3. Ganiev, I.N., Zheleznyak, L.V. (1983) Plotting of liquidus surface of the Al–Si–Ge system by the experimental design simplex method. *Metally*, **4**, 184–187.
4. Zedgenidze, I.G. (1976) *Experimental design to study multi-component systems*. Moscow: Nauka.
5. Scheffe, H. (1958) Experiments with mixtures. *J. Roy. Stat. Soc.*, 20(**2**), 334.
6. Eliot, P. (1987) *Control of eutectic solidification*. Moscow: Metallurgiya.
7. Zhuk, G.V., Trigub, N.P. (2002) New method for dispersing the melt in electron beam units and equipment for its realization. *Advances in Electrometallurgy*, **4**, 15–16.
8. Paton, B.E., Trigub, N.P., Kozlitin, D.A. et al. (1997) *Electron beam melting*. Kiev: Naukova Dumka.
9. Zhuk, G.V., Kozlitin, D.A., Pap, P.A. (1993) Modelling of thermal processes of quick solidification in casting of dispersed melts. *Problemy Spets. Elektrometallurgii*, **3**, 44–49.
10. Nemoshkalenko, V.V., Romanova, A.V., Iliinsky, F.G. (1987) *Amorphous metallic alloys*. Kiev: Naukova Dumka.
11. Golder, Yu.G. (1978) Metallic glasses. *Tekhnologiya Lyog. Splavov*, **6**, 74–93.